REPORT DOCUMENTATION PAGE

Form Approved OMB No. 0704-0188

1. AGENCY USE ONLY (Leave blank)	2. REPORT DATE	3. REPORT TYPE AND DATES COVERED
	Oct 1997	Final Report

4. TITLE AND SUBTITLE

Analysis of Triangular Arrays of Josephson Tunnel Junction

5. FUNDING NUMBERS

F6170897W0207

6. AUTHOR(S)

Prof. Ustinov

7. PERFORMING ORGANIZATION NAME(S) AND ADDRESS(ES)

Department of Physics University of Erlangen-Nuremberg
University of Erlangen-Nuremberg
Erwin-Rommel-Str. 1
Erlangen D-91058
Germany

8. PERFORMING ORGANIZATION REPORT NUMBER

N/A

9. SPONSORING/MONITORING AGENCY NAME(S) AND ADDRESS(ES)

EOARD
PSC 802 BOX 14
FPO 09499-0200

10. SPONSORING/MONITORING AGENCY REPORT NUMBER

SPC 97-4035

11. SUPPLEMENTARY NOTES

12a. DISTRIBUTION/AVAILABILITY STATEMENT

Approved for public release; distribution is unlimited.

12b. DISTRIBUTION CODE

A

13. ABSTRACT (Maximum 200 words)

This report results from a contract tasking Department of Physics University of Erlangen-Nuremberg as follows: The objective of this project is to fabricate planar arrays of small Josephson tunnel junctions and to study their millimeter-wave radiation emission and DC properties.

14. SUBJECT TERMS

Optical Components

15. NUMBER OF PAGES

19

16. PRICE CODE

N/A

17. SECURITY CLASSIFICATION OF REPORT	18. SECURITY CLASSIFICATION OF THIS PAGE	19. SECURITY CLASSIFICATION OF ABSTRACT	20. LIMITATION OF ABSTRACT
UNCLASSIFIED	UNCLASSIFIED	UNCLASSIFIED	UL

Project Report for the period June - October, 1997

on

Analysis of Triangular Arrays of Josephson Tunnel Junctions*

P. Caputo and A. V. Ustinov

Physikalisches Institut III, Universität Erlangen-Nürnberg
D-91054 Erlangen, Germany

* Supported by Air Force Office of Scientific Research (AFOSR)
under Project No. F61708-97-W0207.

Contents

Introduction

This work is aimed to continue the study of dc and rf properties of triangular arrays of Josephson tunnel junctions operating in a magnetic field. Multi-row (two-dimensional) triangular arrays have been proposed as rf oscillator sources with the Josephson junctions transverse to the dc bias current providing the rf output [1, 2]. According to this model, a two-dimensional (2D) triangular array in which a frequency shift along the rows is implemented will generate locked pulse sequences. The first part of this research has been focused on understanding the operating principle of the simplest elements on which the 2D-array is based, i.e. the single triangular cell and the single row array (single frequency oscillator). At the applied magnetic field corresponding to half a flux quantum in every array cell ($f = 1/2$), the junctions transverse to the forcing current (horizontal junctions) oscillate about their equilibrium positions rather than rotating through 2π, yielding rf power with very low levels of higher harmonics. Near $L_s C/3$, the resonance frequency of a 3 junction cell, the entire array can phase lock, producing a measurable radiated power. Although the behavior of these devices was already explained in numerical works done by Yukon and Lin, an experimental evidence was required to assess the expected features. Our experiments done in the first year of this project have shown that radiation is indeed generated by the transverse junctions, and it is a maximum at $f \quad 0.5$.

We have presently performed dc experiments with double row arrays. These systems present more complex behavior, due to the presence of different configurations possible for the circulating currents, which may bring the array into different dynamical states. During summer 1997 we have designed new layouts, which contains single and double row arrays with some variations of previous layouts, in order to explore possibilities of obtaining higher rf power level.

Brief summary of the first year activity (June 1996 - May 1997)

The objective of this research is the experimental study of triangular arrays of Josephson junctions operating in a magnetic field, in order to test the generation of radiation from the horizontal junctions of the array. First we have characterized the dc behavior of discrete single-row and single-cell arrays. As predicted by [1, 2], in the presence of an applied perpendicular magnetic field two steps appear in the I-V curve. The lower voltage step is proportional to the L_JC frequency, where L_J is the Josephson inductance and C is the junction capacitance. The higher voltage step is proportional to the characteristic resonance frequency of a cell $\omega_L = 1/\sqrt{(LC/3)}$, where L is the cell inductance. Both steps are tunable in a range of magnetic field, where the frustration index f is approximately 0.2 - 0.8. Through numerical simulations, Yukon and Lin have shown that operating a triangular array near ω_L can phase lock the entire array and the maximum rf power can be generated. Our objective was to detect radiation from the horizontal junctions of the array operating at the resonance frequency ω_L, and therefore to characterize array properties. In order to make off-chip measurements of the horizontal junction power, we designed a fin-line antenna and coupled it to the horizontal junctions of arrays. To avoid signal reflections and therefore power losses, the impedance matching between the horizontal junction row of the array and the microstripline of the antenna has been optimized. High frequency properties were investigated using two room temperature superheterodyne receivers, for 75 GHz and for the band 80 - 120 GHz. Radiation measurements on a 12 cell triangular array confirmed that an rf voltage is developed in the junctions transverse to the forcing current. We observed that radiation power is a maximum at $f = 0.5$ and drops as soon frustration is changed from 0.5, which confirms a change in the phase relationships between the horizontal junctions as the magnetic field is tuned. Detailed description of experimental technique and results is contained in Ref.[3, 4].

New chips have been prepared at Hypres foundry. The designs contain arrays with different number of cells and different cell size. In addition, a chip with shunted junctions has been fabricated. The following tasks are planned:

- to test the scaling of rf power in single-row arrays with the number of emitting junctions and to make measurements of the linewidth of the emitted radiation.
- to make comparative study of triangular arrays with different damping in the junctions and with different geometry of the cells (square cells versus triangular cells). in order to investigate the possibility to enhance the rf power.
- to make systematic DC and RF characterization of two-row arrays.

Characterization of a two-row array

Array parameters

Several different two-row arrays with basic cell having 3 junctions were designed and fabricated with Nb-Al_xO_y-Nb technology [7]. The elementary cell size of devices contained in this layout was designed to be $160\,\mu m^2$. The arrays we studied consist of one row array (1×12 cells) and of two row array (2×12 cells). In Fig. 1(a) a double row array is sketched. The two rows A and B are biased in series and the voltage response across each row is measured separately, so that two single row I-V curves can be monitored simultaneously. Placed symmetrically with respect to the two rows, a control line goes along the common horizontal junction line of the array. The control line is formed in the upper Nb layer and insulated from the top junction electrode by a 500 nm thick SiO_2 layer, making it possible to pass a control current I_{cl} through the line without changing the bias current I_b in the junctions (see Fig. 1(b)). Samples consist of underdamped Nb-Al_xO_y-

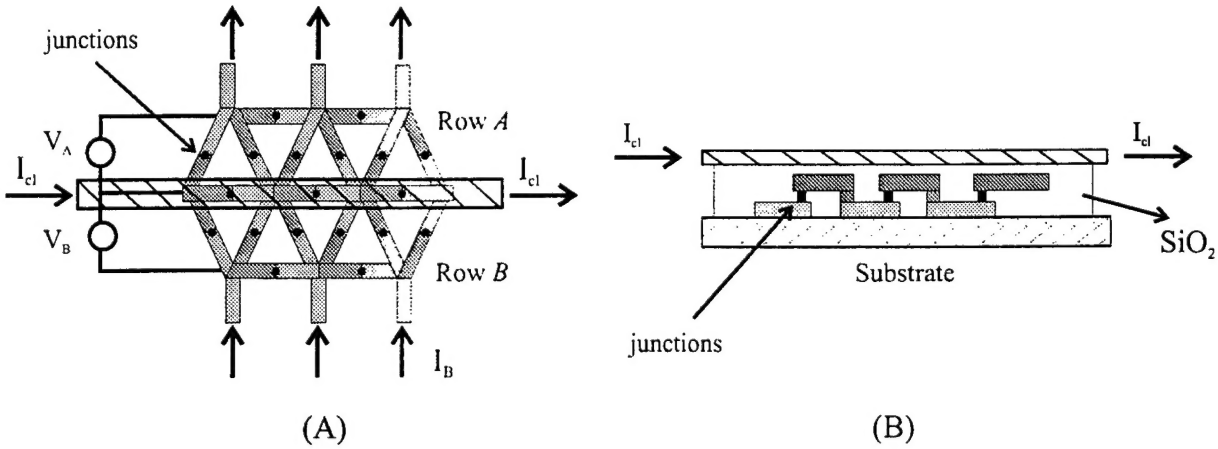

Figure 1: Schematic top view (a) and cross view (b) of a double row array made of 5×2 cells and with the control line.

Nb junctions having a critical current density of about 1000 A/cm^2. The good level of fabrication technique results in a low spread of junction parameters: in fact the two rows

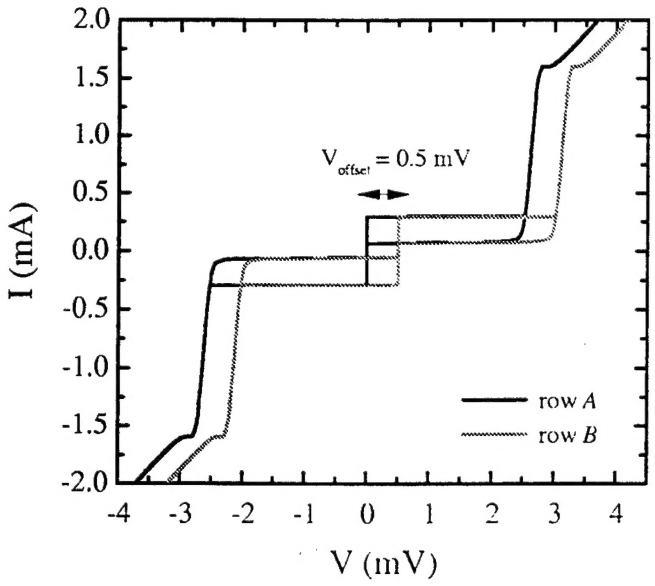

Figure 2: I-V curve of the two row array (sample 2844G#3). The voltage across each row is read independently. An offset of 0.5 mV is applied to the second curve.

have very similar electrical parameters, like critical currents, subgap resistances, normal resistances and gap voltages. In Fig. 2 the typical I-V curve of the array is shown, with a voltage offset of 500 μV in one row. In Table we listed the geometrical and electrical parameters of the sample 2897A#7. The junction critical current I_c has been calculated from the array critical current. The cell inductance L_s is estimated as $L_s \approx 1.25\mu_0 A^{1/2}$, where μ_0 is the magnetic permeability and A the cell area. The discreteness parameter is $\beta_L = 2\pi L_s I_c/\Phi_0$, where Φ_0 is the magnetic flux quantum.

By means of an external coil a perpendicular magnetic field H is applied to the array. The magnetic field is expressed in terms of frustration f, which is the applied magnetic flux per unit cell, normalized to the flux quantum Φ_0. The control line gives an additional possibility to tune in opposite directions the effective frustration of each row, creating different magnetic flux densities in the two rows. In this way, one breaks the symmetry between the rows and can study the stability of the dynamical states in the array.

dc measurements

We will give here a description of the dc behavior of the double row array in the presence of an external magnetic field, provided either by the external coil or by the control line. We have studied both the statics and dynamics of the two row arrays under these two different ways of injecting the magnetic field. In particular, the stability of voltage locked

Sample no.	#7, 12 × 2 cells
Junction size, S	$9\,\mu m^2$
Cell size, A	$160\,\mu m^2$
Critical current density, J_c	$1050\,A/cm^2$
Junction critical current, I_c	$44\,\mu A$
Junction normal resistance, R_N	$21\,\Omega$
Junction capacitance, C	340 pF
Cell inductance, L_s	20 pH
Josephson inductance, L_J	7.5 pH
Discreteness parameter, β_L	2.6
McCumber parameter, β_c	1800

Table 1: Parameters of the sample 2897A#7 at $T = 4.2\,K$.

states in the two rows has been investigated as a function of current passed in the control line. All measurements have been performed at temperatures above 6 K, because at lower temperatures the steps were not stable due to relatively large β_L. Also, as the temperature affects the damping in the junctions, the parameter region (f, I_d, I_b) where the steps are stable depends on temperature. We found out that the decrease of temperature moves more narrow the parameter range where the steps are stable. In terms of the discreteness parameter β_L, we observed stable dynamical states only when β_L is of about 1, or smaller.

We first characterize the single row array which has the same elementary cell size as the double row array ($A = 160\,\mu m^2$) and the same number of cells in the row (12×1). In the presence of field, two resonances appear on the I-V curve. In Fig. 3 we reported the I-V curves at increasing values of f, and the two steps are marked as V_1 and V_2. The voltage position of the steps is tuned by field. These resonances have already been studied in single row array [5, 3] and described in previous studies [1, 2]. The lower step V_1 is proportional to the L_JC frequency, while the upper step V_2 corresponds to the $L_sC/3$ resonance frequency of the triangular cell. In particular, the step V_2 has been attributed to a realized dynamical checkerboard pattern in the array [6]. Both steps are characteristics of single cell, and their voltage does not change with number of cells in the array. Moreover, measurements of different cell size arrays show that V_2 depends on the cell size, in contrast to V_1. The step V_1 appears approximately in the frustration interval 0.2 - 0.8 and reach the maximum voltage value at $f = 0.5$. The voltage of step V_2 is slightly tunable by field, and has the maximum current amplitude at $f = 0.5$.

In Fig. 4 we show a typical $I_c(H)$ dependence at $T = 4.2\,K$. The pattern shows a series of maxima at almost regular field interval. Maxima are located at field values which correspond, in average, to an integer number of fluxons per cell. At this temperature,

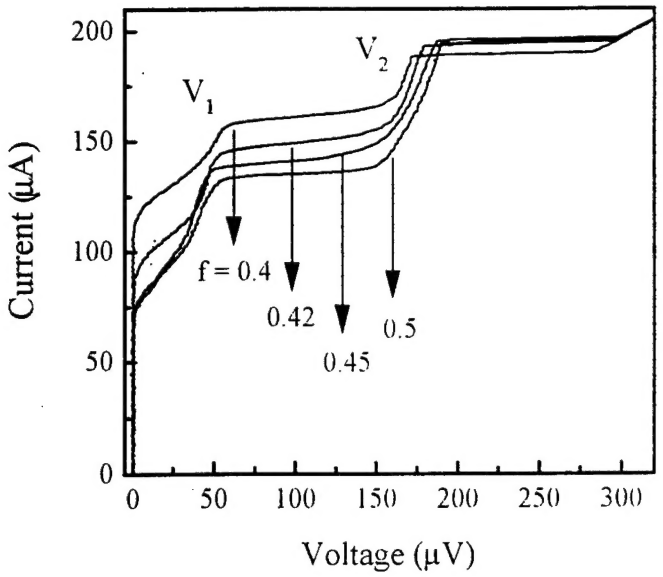

Figure 3: Overlapped I-V curves of one row array (sample 2897A#5) at different values of frustration f. When changing f, the lower step V_1 moves in the range 0 - 60 μV, the upper step V_2 moves in the voltage range 160 - 190 μV. Here the McCumber parameter β_c is ≈ 500.

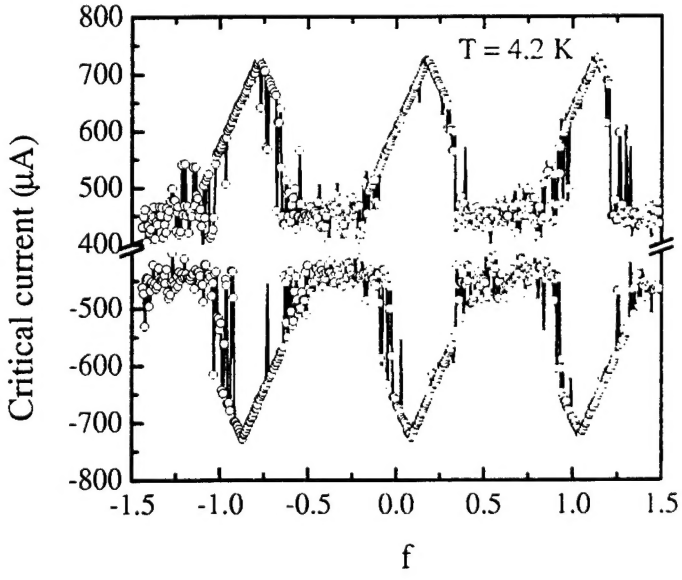

Figure 4: $I_c(H)$ dependence at $T = 4.2$ K for array 2897D#5.

the array critical current I_c is never suppressed below 450 μA, which is well above the maximum current of the two steps on I-V curve, therefore these steps are never stable at these temperatures. The steps stably appear only when the temperature is high enough so that f modulates the Josephson current I_c below their maximum current. In terms of McCumber parameter, defined as $\beta_c = 2\pi I_c R_{sg}^2 C/\Phi_0$, the step becomes stable when $\beta_c \approx 500$.

In Figs. 5 and 6 the voltage positions of the steps are plotted as a function of f for two different temperatures. The $I_c(f)$ dependence is reported on the same plots as a reference. The lower step V_1 has the maximum voltage at about 80 μV, and the upper step V_2 at about 190 μV. The step voltage V_1 depends on the temperature, and its saturation value (at $f = 0.5$) decreases with increasing the temperature. This is in agreement with the interpretation related to the Josephson inductance that has been given to the nature of the step [1].

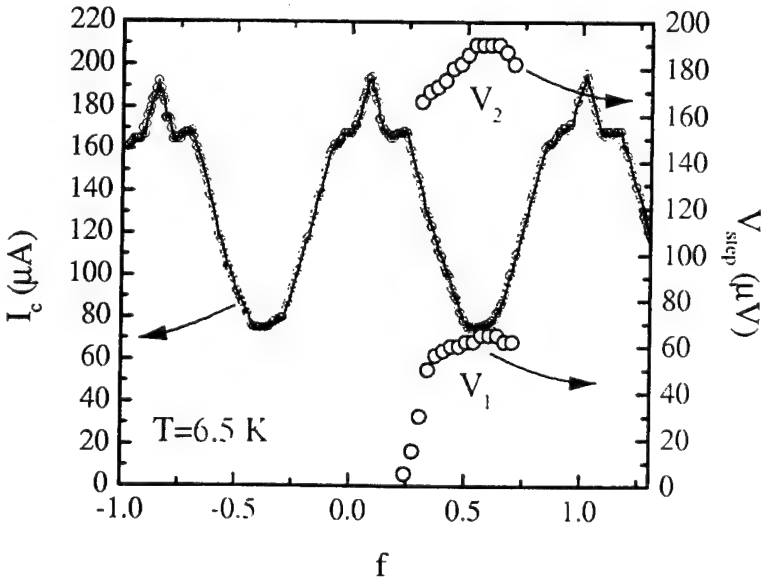

Figure 5: $I_c(H)$ dependence and voltage position of the resonances V_1 and V_2 at $T = 6.5$ K for array 2897A#5.

The double row array shows similar $I_c(H)$ dependencies, with the maxima spaced at almost regular field intervals. In Fig. 7 we report the pattern at $T = 4.2$ K for the two rows and for both current polarities. One row shows sudden jumps to higher currents. This is the artifact of the measurements technique that, at certain frustration values, first the two rows switch together to high voltages but then one of them *looses* the locking with the other row and jumps to a state around 10 μV or less, which is read from the acquisition data program as "zero voltage current". Several $I_c(H)$ dependencies were recorded also at different values of the current I_{cl} in the middle control line. With increasing I_{cl}, the

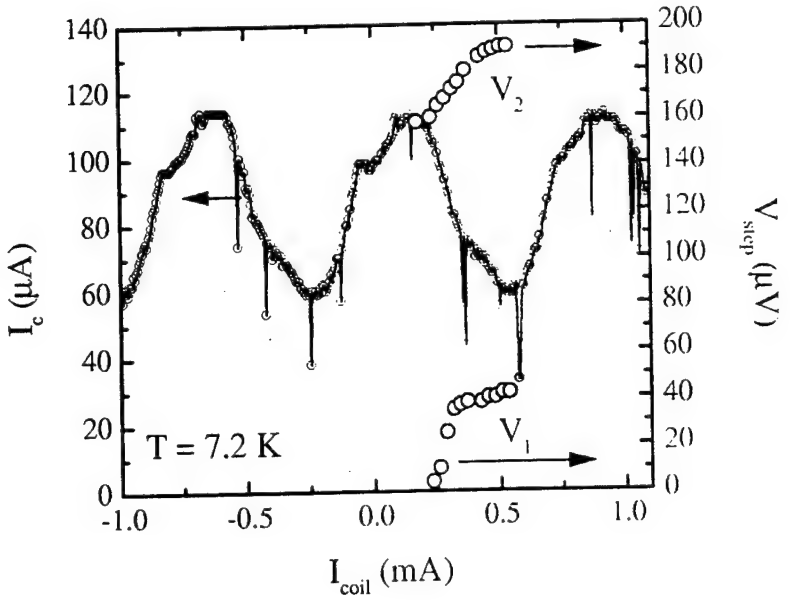

Figure 6: $I_c(H)$ dependence and voltage position of the resonances V_1 and V_2 at $T = 7.2\,\mathrm{K}$ for array 2897A#5.

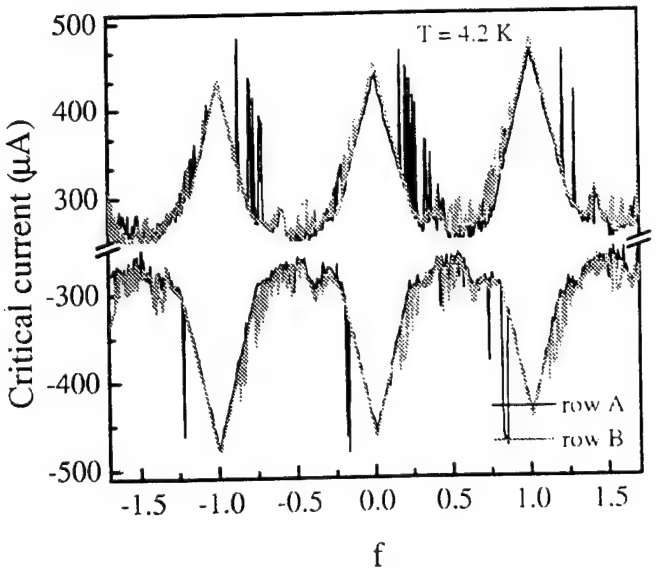

Figure 7: $I_c(H)$ dependence at $T = 4.2\,\mathrm{K}$ for the double row array 2897A#7. The curves of row A and row B are overlapped.

peak of I_c at $f = 0$ in one row moves towards positive f, while the peak of the other row is shifted towards negative f. This corresponds to the shift of the effective frustration seen by each row as consequence of the extra field given by I_{cl}. The shift of the peak is linear with the current I_{cl}. At a certain value of control current ($I_{cl} \approx 137\,\mu$A) the peak that without control current was at $f = 0$ is shifted to $f = 1$ in row A ($f = -1$ in the row B), indicating that at this moment one fluxon more per cell is added (subtracted) in the row A (B) due to the field induced by I_{cl}.

Depending on the value of f, we can distinguish 3 kinds of I-V curves of the array. In Fig. 8 the I-V curves corresponding to the various dynamical regimes are plotted. The curves are marked by the values of f at which they have been traced, and the steps are referred to as V_1, V_2 and V_4. For $(n - 0.15) \leq f \leq (n + 0.15)$, $n = 0, \pm 1, \ldots$, the I-V curve shows the large resonant step V_4 which has the asymptotic voltage $V \approx 280\,\mu$V. This resonant step does not depend on magnetic field and temperature. There are only

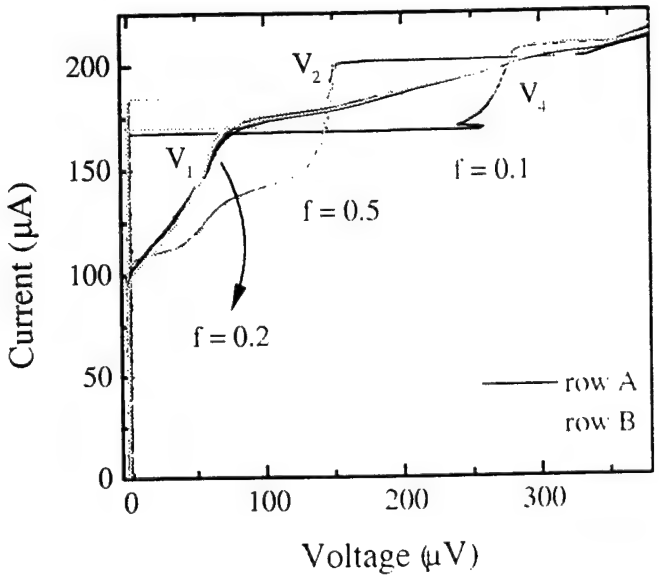

Figure 8: Overlapped I-V curves of array 2897A#7 showing different regimes at various values of f. The curves of row A and row B are overlapped.

slight voltage variations at the bottom of the step, mainly due to both the field and temperature dependence of the McCumber slope from which the step merges. In Fig. 9(a) several I-V curves at $f = 0$ are shown at different temperatures. At each temperature the voltages across the two rows are read separately. At $f = 0$, if the temperature is high enough to suppress the Josephson current I_c below the maximum current of the step (I_c^3), there is a direct transition from the zero voltage state to the step V_4. When the McCumber parameter is higher than ≈ 1300, this step is not stable. It is present when $400 \leq \beta_c \leq 1300$. However, increasing f above 0.1 the jump to the step does

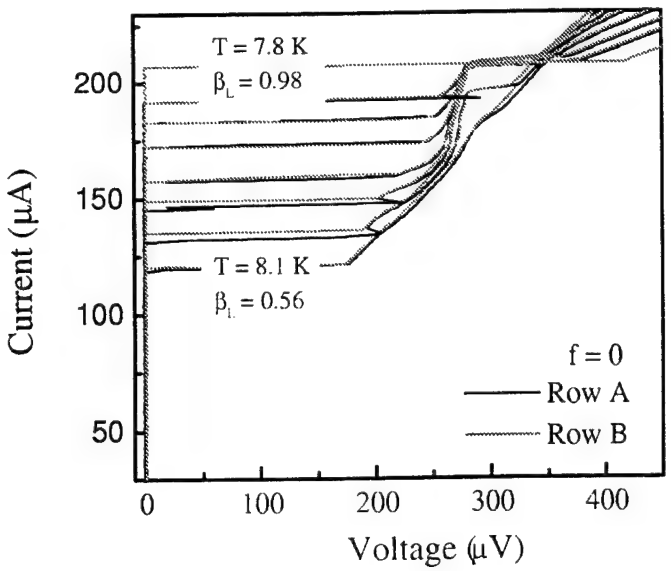

Figure 9: Overlapped I-V curves of array 2897A#7 at $f = 0$ and for various temperatures in the range $T = 7.8 - 8.1$ K. In this temperature range the McCumber parameters goes from ≈ 400 to ≈ 1300.

not take place directly from I_c, but instead it goes through the plasma resonance step V_1 which is present at these frustration values. The step V_4 appears at a voltage which scales with the size of the elementary cell. In fact, for the array with cell of $160\,\mu\text{m}^2$ the step is at $V_4 \approx 280\,\mu$V, and for the cells of $250\,\mu\text{m}^2$ the step is shifted to $V_4 \approx 240\,\mu$V. This step is never observed in the single row arrays. When biased on the step V_4, the two rows are almost always voltage synchronized, indicating the existence of locked dynamical states in the rows. However, we observed that when the critical current of the rows are slightly different their switch from $V = 0$ takes place to two slightly different voltages, which eventually merge at higher bias. This behavior is met when using the control line, because current I_{cl} creates opposite magnetic fields in the two rows leading to two different critical currents. In Fig. 10 (a-b-c-d-e-) the sequence of I-V curves at different values of control current I_{cl} is reported. When $I_{cl} = 0$ (a), the two curves overlap completely and the two rows simultaneously go from the zero voltage state to the same voltage state V_4. As soon as $I_{cl} \neq 0$, the two critical currents split due to the effective frustration different from row to row. Thus, the two rows switch from $V = 0$ to two slightly different steps. In particular, the row with lower I_c switches to a higher voltage state $V > V_4$, and follows this branch until also the other row switches to the voltage state. At this moment, the row that has switched first is *pulled* back to the resonance V_4 (see Fig. 10(b)), and both rows stay at equal voltages until eventually they synchronously switch to the McCumber branch. Plots (c-d-e) show this behavior at various I_{cl} values. As one can see, further

increases of I_{cl} enlarge the region where the two rows are not locked, until I_{cl} creates a field that destroys the resonances, see Fig. 10(f).

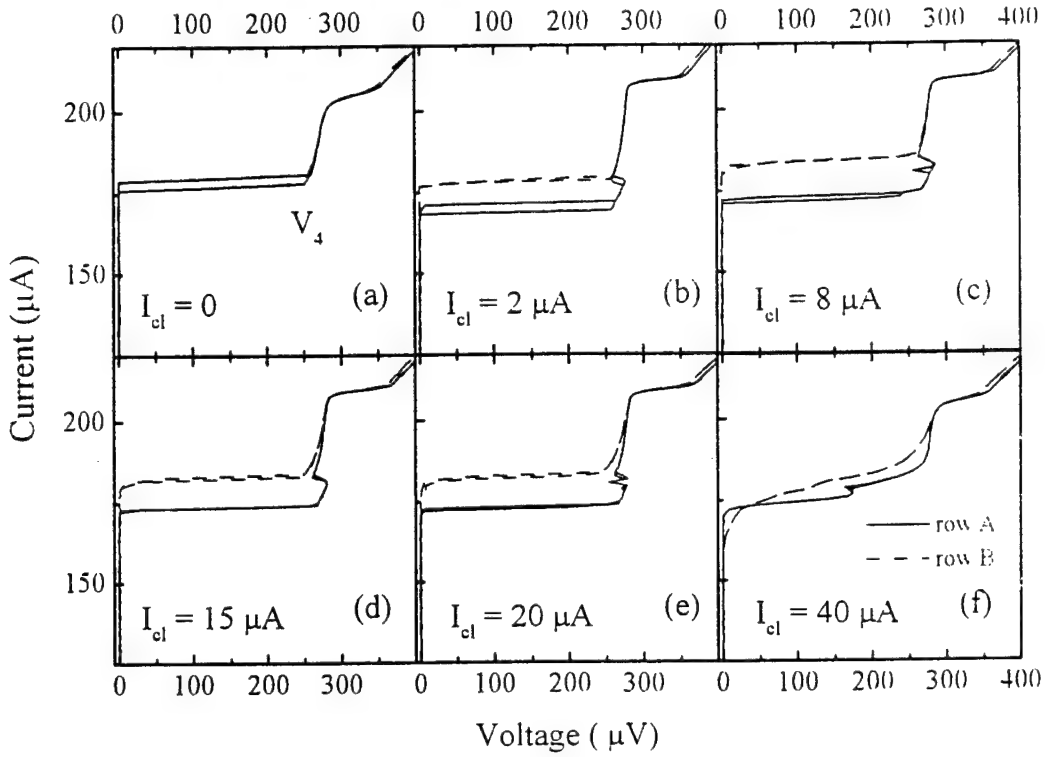

Figure 10: The plot sequence (a)...(f) shows the I-V curves of the two rows of array 2897A#7 at different values of current I_{cl} in the control line.

At larger values of f the step V_4 does not exist and two steps V_1 and V_2 appear at lower voltages in the I-V curve. The field dependence of the voltage position of the step V_1 is similar to the one observed in single row arrays: in fact the step appears only in the presence of a magnetic field, and reaches the saturation voltage (and the maximum stability) at frustration one-half. The maximum voltage of V_1 is $\approx 90\,\mu$V, and it depends on the temperature. This step is reported in Fig. 8 by the curve marked "$f = 0.2$" and the step is named V_1.

The way the step V_2 is modulated by magnetic field for the double row array has a different behavior from that in single row arrays. While in the single row arrays this step is tuned smoothly by f, in the two row arrays the step V_2 has a rather steep main branch (marked as V_2 in Fig. 8) which eventually evolves in the more smooth behavior. The step exists in a large range of f, and its current amplitude is modulated by f. In Fig. 11 we report several I-V curves which reproduce the profile of this step at different f. Row A (black line) and row B (gray line) are recorded simultaneously. We can see the large resonance at $V \approx 150\,\mu$V. Here the McCumber parameter is ≈ 300. Approaching f 0.5

the amplitude of step V_2 progressively decreases and the step evolves into the higher voltage state V_3. Further increasing of f slightly moves the step V_3 up to the maximum position $V = 180\,\mu$V reached at $f = 0.5$. We notice that this saturation voltage is the

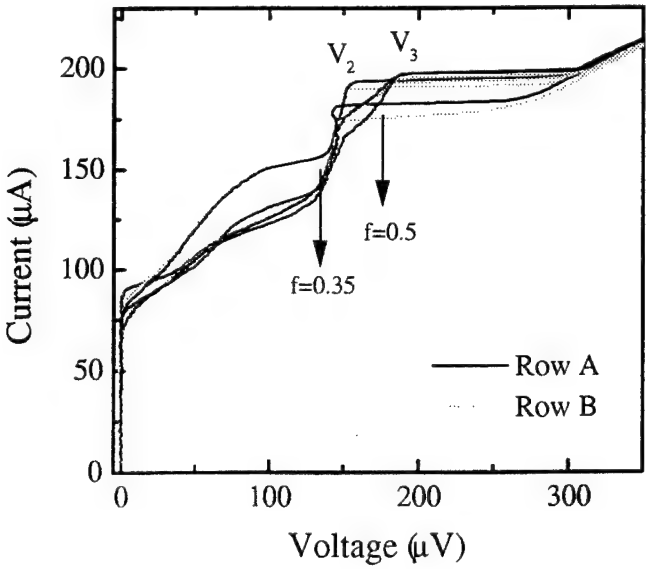

Figure 11: I-V curves showing the behavior of the two row array 2897A#7 around $f = 0.5$. Row A and row B are recorded simultaneoulsy and plotted. At the working temperature, β_c is ≈ 300.

same as reached at $f = 0.5$ in the one-row array. Fig. 12 presents a comparison of the I-V curves for the single row and double row arrays at $f = 0.5$. The I-V curve of the double row array is shown when the resonance V_2 is present and has its maximum current amplitude, i.e. at a bit lower frustration than 0.5. Also, it is hard to distinguish between the two rows, since they overlap almost completely.

In Fig. 13 we compare the dependence of the current amplitude of the resonances as a function of f. The plot also contains the $I_c(f)$ dependence for the reference. All currents are referred to the same current axes. At a fixed value of frustration two current points are reported, which correspond to the minimum and the maximum current of the step. The resonance V_4 which exists at low values of f is marked with solid squares. Its current amplitude has a maximum at $f = 0$, and rapidly decreases with increasing f. The I-V curve corresponding to the point marked "(a)" is shown in Fig. 14(a). Increasing f, the resonances V_1 and V_2 appear in the I-V curve. In the plot of Fig. 13 we do not report the resonance V_1, because it is the standard plasma resonance described above, which behaves in the same way in both single and double row arrays. The current amplitude of V_2 is marked with solid triangles. Its current amplitude increases with increasing f, but at certain values of $f \propto I_{coil}$ its amplitude start to decrease and the step evolves in the

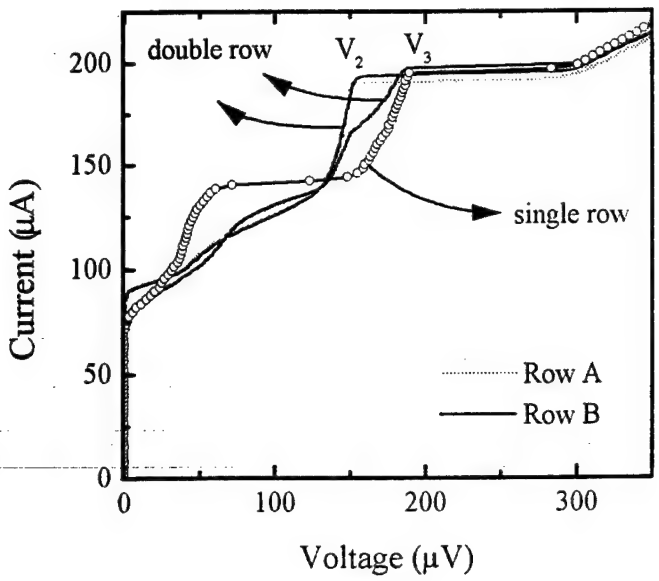

Figure 12: I-V curves showing the behavior of the two row array 2897A#7 around $f = 0.5$. The curve marked by open circles is the single row array 2897A#5 at $f = 0.5$. The two continuous curves are referred to the double row array at values of f approaching 0.5. Both rows A and B are plotted.

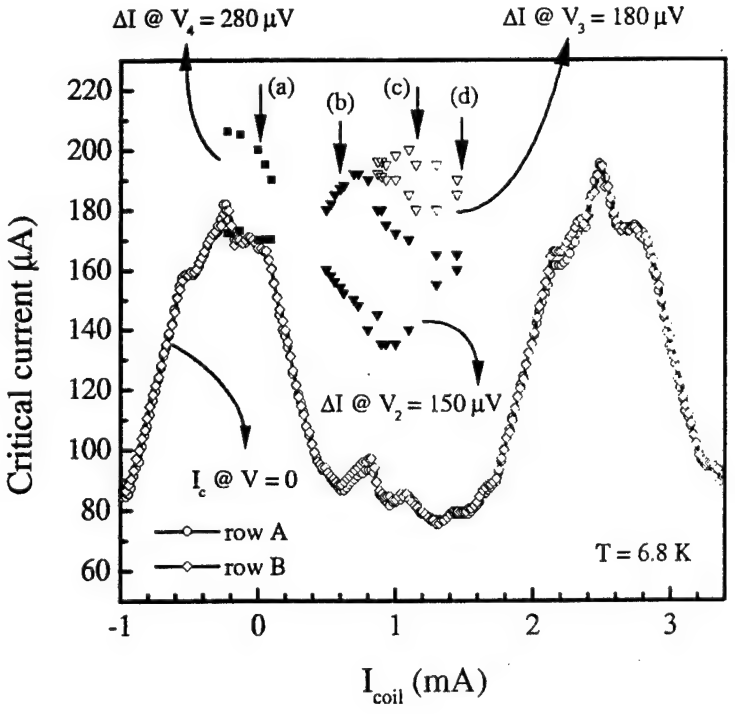

Figure 13: Dependence of the current amplitude of the resonances V_2 (solid triangles), V_3 (open triangles) and V_4 (solid squares) as a function of f. The Josephson critical current is reported as reference. The I-V curves corresponding to the points marked as (a)..(d) are separately reported in Fig.14.

branch V_3, marked in the plot by open triangles. The amplitude of V_3 has a maximum at $f = 0.5$. The points marked with (b), (c) and (d) correspond to the plots of Fig. 14(b)-(c)-(d). We note that the described behavior is always present is both rows, unless we

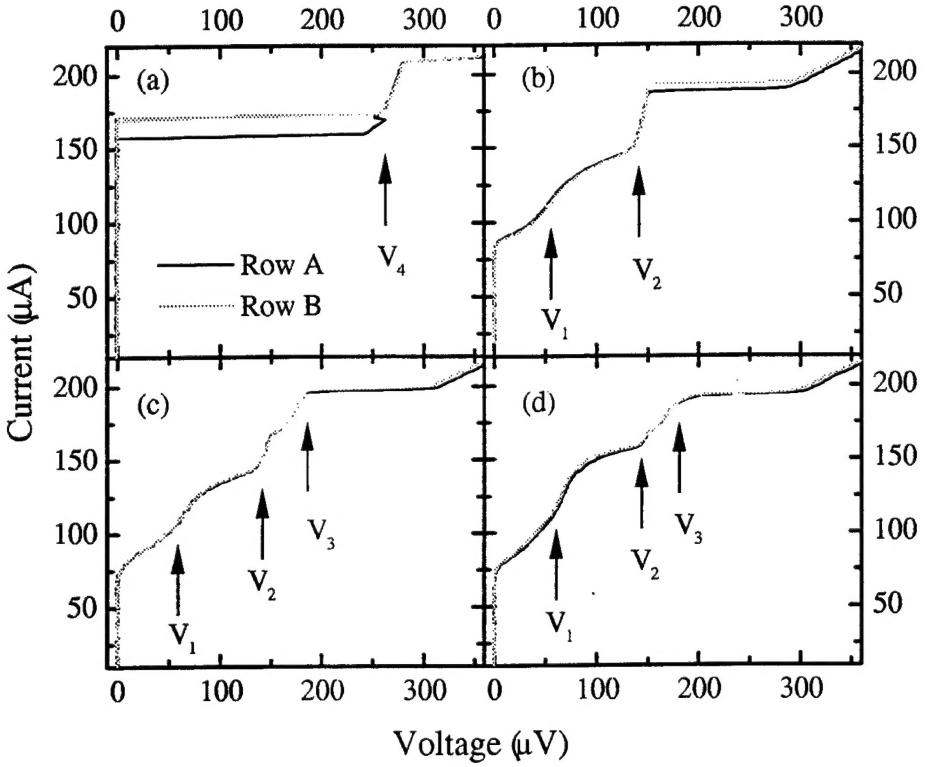

Figure 14: *I-V* curves corresponding to the points marked as (a)..(d) in Fig.13.

use the control line to break the field symmetry. The resonance V_2 exists in a quite large interval of f. To see this we plot its voltage position as a function of f (see Fig. 15). We remark that the splitting of the resonance V_2 is never observed in the single row arrays, but it is indeed a feature of the double row arrays. However, if some current in the control line is passed when the resonance V_2 is present in both rows, we can bring one row in a state having still the resonance V_2 and tune the other row into a state with the resonance V_3. This is finally shown in Fig. 16.

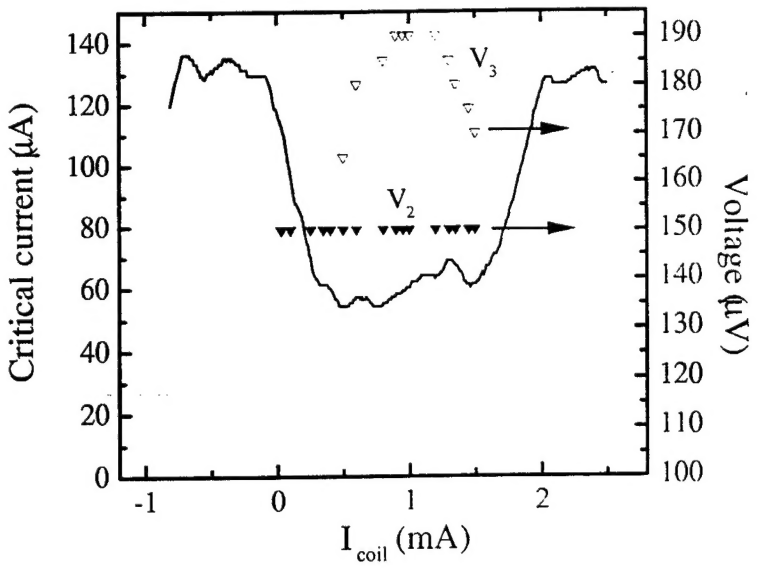

Figure 15: $I_c(H)$ dependence and voltage position of the resonances V_2 (solid triangles) and V_3 (open triangles) for the two row array (2897A#7).

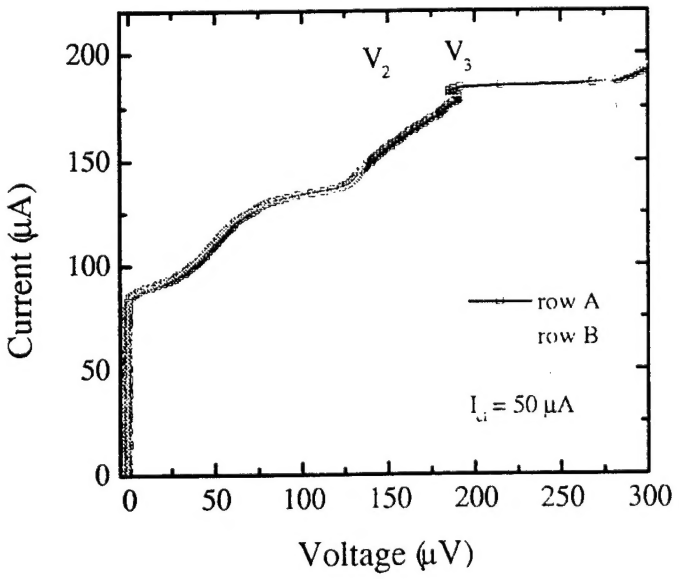

Figure 16: I-V curves of the two rows when a current $I_{cl} = 50\,\mu$A is passed in the control line.

Summary

We have performed systematic dc measurements of double-row arrays. In the presence of an applied perpendicular magnetic field (with same orientation in both rows), a synchronized dynamics takes place in the two rows. The double row arrays show resonances which are not present in the single row arrays. We observed a new high voltage resonance which appears at almost zero frustration. In addition, at $f = 0.5$ the geometrical resonance splits in two steps. Voltage locked states of the two rows can be controlled by a current passing through the control line along the central axis of the array. In this way, it is possible to realize different dynamics in the two rows, which brings to two different I-V curves.

Bibliography

[1] S. P. Yukon and N. C. Lin in *Macroscopic Quantum Phenomena and Coherence in Superconducting Networks*, (Singapore, 1995), p. 351.

[2] S. P. Yukon and N. C. Lin, IEEE Trans. Appl. Sup. to appear 1997.

[3] P. Caputo, A. E. Duwel, T. P. Orlando, A. V. Ustinov, N. C. Lin, and S. P. Yukon. Proc. of ISEC'97, Berlin, June 1997, p. 180.

[4] P. Caputo and A. V. Ustinov, *Analysis of Triangular Arrays of Josephson Tunnel Junctions* (Internal Report).

[5] A. Duwel et al., unpublished.

[6] M. Barahona, E. Trias, T. P. Orlando, A. E. Duwel, H. S. J. van der Zant, S. Watanabe, and S. H. Strogatz, Phys Rev B **55**, R11989 (1997).

[7] HYPRES Inc., Elmsfort, NY 10523.